Electronic Supplementary Material (ESI) for Journal of Materials Chemistry A.
This journal is © The Royal Society of Chemistry 2022

Electronic supplementary information

Enhancing exciton diffusion by reducing energy disorder in organic solar cells

Peiyao Xue,[a] Adiel M. Calascibetta,[c] Kai Chen,[d] Karen E. Thorn,[d] Yiting Jiang,[a] Jiangjian Shi,[e] Boyu Jia,[a] Mengyang Li,[f] Jingming Xin,[g] Guilong Cai,[h] Rui Yang,[i] Heng Lu,[a] Sara Mattiello,[c] Yao Liu,[i] Zheng Tang,[f] Wei Ma,[g] Xinhui Lu,[h] Qingbo Meng,[e] Justin M. Hodgkiss,[d] Luca Beverina,[c] Ray P. S. Han,[j] and Xiaowei Zhan[a,b,*]

[a]School of Materials Science and Engineering, Peking University, Beijing 100871, China. *E-mail address*: xwzhan@pku.edu.cn

[b]Key Laboratory of Eco-functional Polymer Materials of Ministry of Education College of Chemistry and Chemical Engineering, Northwest Normal University, Lanzhou 730070, China

[c]Department of Materials Science, State University of Milano-Bicocca, Via Cozzi 55, Milano, Italy

[d]MacDiarmid Institute for Advanced Materials and Nanotechnology, School of Chemical and Physical Sciences, Victoria University of Wellington, Wellington 6010, New Zealand

[e]CAS Key Laboratory for Renewable Energy, Beijing Key Laboratory for New Energy Materials and Devices, Institute of Physics, Chinese Academy of Sciences, Beijing 100190, China

[f]Center for Advanced Low-Dimension Materials, State Key Laboratory for Modification of Chemical Fibers and Polymer Materials, College of Materials Science and Engineering, Donghua University, Shanghai 201620, China

[g]State Key Laboratory for Mechanical Behavior of Materials, Xi'an Jiaotong University, Xi'an 710049, China

[h]Department of Physics, The Chinese University of Hong Kong, New Territories 999077, Hong Kong, China

[i]Beijing Advanced Innovation Center for Soft Matter Science and Engineering, State Key Laboratory of Chemical Resource Engineering, Beijing University of Chemical Technology, Beijing 100029, China

[j]Jiangzhong Cancer Research Center, Jiangxi University of Chinese Medicine, Nanchang 330004, China.

Materials

2,5-Dibromo-*N*-(2-ethylhexyl)-3,4-thiophenedicarboximide was purchased from TCI, 1,4-dibromo-2,5-didecyloxyphenylene was purchased from Sigma Aldrich, and the palladium catalysts were purchased from Apollo Scientific. PM6 was purchased from Solarmer Materials Inc., Y6 and PNDIT-F3N were purchased from EflexPV Inc., PEDOT:PSS (CLEVIOS^{TM} PVP AI 4083) was purchased from Heraeus Inc. Unless stated otherwise, all chemical reagents and solvents were used without further purification.

Synthesis of 2,5-didecyloxyphenylene-1,4-bis(4,4,5,5-tetramethyl-1,3,2-dioxaborolate)

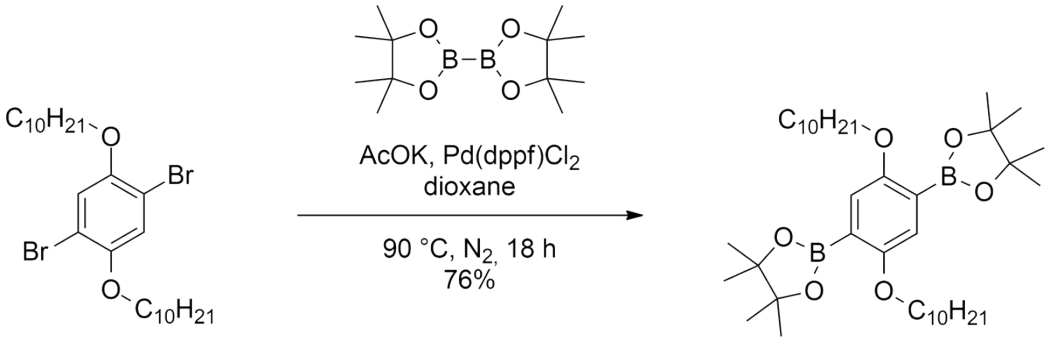

Glassware (a 100 mL dual-necked round-bottom flask, stirrer and condenser equipped with tubing adapter) was carefully dried before use by warming up to 120 °C overnight in oven. Anhydrous AcOK was maintained at 120 °C overnight before use as well. The system was subsequently put under vacuum while still hot and allowed to cool down to room

temperature under vacuum to avoid water condensation within the reaction flask. The system was put under nitrogen atmosphere by mean of a Schlenk line, and all the reagents were added in the reaction flask while maintaining a positive stream of nitrogen. Reagents were added in the following order: AcOK (1.074 g, 10.94 mmol), 1,4-dibromo-2,5-didecyloxyphenylene (1.000 g, 1.711 mmol), bis(pinacolato)diboron (1.390 g, 5.474 mmol), Pd(dppf)Cl_2 (53.0 mg, 0.0724 mmol). After addition of reagents, the reaction flask was purged three times by performing vacuum/nitrogen cycles. Finally, anhydrous dioxane (4 mL) was added and the flask was heated up to 90 °C for 18 hours. The reaction was cooled down to room temperature, diluted with toluene and filtered on Celite. Solvent was evaporated under reduced pressure, and the raw product was finally purified by crystallization with methanol. The solution was cooled down to -20 °C overnight before collecting the crystallized product by filtration. White powder, 840 mg, 76% yield. ^{1}H NMR (400 MHz, $CDCl_3$): δ 7.08 (s, 2H), 3.93 (t, J = 6.3 Hz, 4H), 1.78-1.71 (m, 4H), 1.53-1.46 (m, 4H), 1.34 (s, 24H), 1.32-1.24 (m, 24H), 0.88 (t, J = 7.0 Hz, 6H).[S1] ^{13}C NMR (100 MHz, $CDCl_3$): δ 157.69, 119.94, 83.41, 69.79, 31.88, 29.69, 29.67, 29.61, 29.54, 29.33, 26.07, 24.84, 22.65, 14.08.

Synthesis of AC174

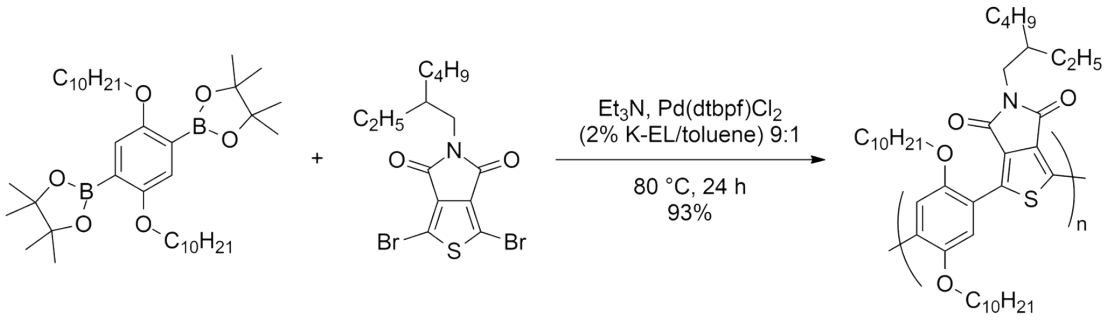

AC174 was synthesized by Suzuki-Miyaura polycondensation in micellar conditions[S2] between 2,5-didecyloxyphenylene-1,4-bis(4,4,5,5-tetramethyl-1,3,2-dioxaborolate) and 2,5-dibromo-*N*-(2-ethylhexyl)-3,4-thiophenedicarboximide. In a 10 mL round-bottom vial, 2,5-didecyloxyphenylene-1,4-bis(4,4,5,5-tetramethyl-1,3,2-dioxaborolate) (160 mg, 0.249 mmol), 2,5-dibromo-*N*-(2-ethylhexyl)-3,4-thiophenedicarboximide (105 mg, 0.248 mmol) and Pd(dtbpf)Cl_2 (6.0 mg, 0.0092 mmol) were weighted, then 1.0 mL of K-EL emulsion (composed of aqueous 2 wt% Kolliphor EL solution and toluene in 9:1 volume ratio) was added. The mixture was allowed to stir for five minutes before addition of Et_3N (151 mg, 1.49 mmol). Immediately after the addition of the base, the mixture was warmed in a pre-heated silicone bath at 80 °C and allowed to react for 24 hours. At the end of the reaction, the mixture was diluted with 10 mL of methanol and transferred into a cellulose thimble to be subjected to Soxhlet extraction with methanol, acetone, and heptane. 151 mg of final material (93% yield) was recovered from the heptane fraction. ^{1}H NMR (400 MHz, $CDCl_3$): δ 8.47 (s, 1H), 8.20 (s, 1H), 4.63-4.13 (m, 4H), 3.61-3.08 (m, 2H), 2.36-1.83 (m, 4H), 1.95-1.75 (m, 1H), 1.46-1.16 (m, 36H), 1.04-0.78 (m, 12H). Anal. calcd for $C_{42}H_{67}NO_4S$ (%): C 73.96, H 9.90, N 2.05; found: C 73.28, H 9.22, N 2.01.

The number-average (M_n) and weight-average (M_w) molecular weights were determined by size exclusion chromatography (SEC) and calibrated against polystyrene standards. The sample for SEC analysis was measured at 35 °C on a Waters 510 HPLC system equipped with a Waters 2410 refractive index detector. THF was used as eluent. The sample to analyse (volume 200 μL, 2 mg mL^{-1} in THF) was injected into a system of columns connected in

series (Ultrastyragel models HR 4, HR 3, and HR 2, Waters), and the analysis was performed at a flow rate of 0.5 mL min^{-1}. M_n = 17.0 kg mol^{-1}, M_w = 38.6 kg mol^{-1}, M_w/M_n = 2.27.

Device fabrication

All the devices are based on the conventional sandwich structure, indium tin oxide (ITO) glass/PEDOT:PSS/active layer/PNDIT-F3N/Ag. First, the patterned ITO glass (sheet resistance = 15 Ω $□^{-1}$) was precleaned in the ultrasonic bath with de-ionized water, acetone and isopropanol, respectively. The pre-cleaned ITO glass was treated by ultraviolet-ozone chamber (UVO) (Jelight Company, USA) for 15 min. Then, the PEDOT:PSS layer (*ca.* 30 nm) was spin-coated at 3000 rpm onto the ITO glass, followed by baking at 150 °C for 15 min. After that, the photoactive layer consisting of donor mixture:Y6 solution (14.7 mg mL^{-1} in total, 0.5% *v/v* 1,8-diiodooctane (DIO), chloroform) was spin-coated at 3000 rpm onto the PEDOT:PSS layer (*ca*. 100 nm, measured by profilometer (Dektak XT)), followd by annealing at 100 °C for 5 min. The ratio of donors and acceptor is 1:1.2. The amount of AC174 in donors varies from 0, 5, 10, 20, 50 to 100%. After that, the PNDIT-F3N solution (0.5 mg mL^{-1} in methanol) was spin-coated onto the active layer at 2000 rpm. Finally, Ag electrode layer (*ca.* 80 nm) was then evaporated onto the PNDIT-F3N layer under vacuum (*ca.* 10^{-5} Pa). The measured area of the device was 4 mm^2 (2 mm × 2 mm).

Device characterization

The current density-voltage (*J-V*) curves were measured using a computer-controlled B2912A Precision Source/Measure Unit (Agilent Technologies). An XES-70S1 (SAN-EI Electric Co., Ltd) solar simulator (AAA grade, 70 × 70 mm^2 photobeam size) coupled with

AM 1.5G solar spectrum filters was used as the light source, and the optical power at the sample was 100 mW cm^{-2}. A 2 × 2 cm^2 monocrystalline silicon reference cell (SRC-1000-TC-QZ) was purchased from VLSI Standards Inc. The external quantum efficiency (EQE) spectra were measured using a Solar Cell Spectral Response Measurement System QE-R3011 (Enlitech Co., Ltd.). The light intensity at each wavelength was calibrated using a standard single crystal Si photovoltaic cell.

Optoelectrical characterization

The UV-vis absorption spectra were measured on UV3600Plus spectrophotometer in solution (dichloromethane) and thin films (on a quartz substrate). The steady-state photoluminescence spectra were recorded on FLS980 fluorescence spectrophotometer (Edinburgh Instrument Co., Ltd.). Ultraviolet photoelectron spectrometer (UPS) measurements were performed on the AXIS Supra X-ray photoelectron spectrometer. The HOMO energy (E_{HOMO}) was obtained directly from UPS using the following formula:

$$E_{HOMO} = E_{cutoff} - E_{onset} - hv \qquad \text{(S1)}$$

where hv = 21.22 eV, E_{cutoff} and E_{onset} are binding energy at cutoff and onset positions of the UPS spectra, respectively. The LUMO energy (E_{LUMO}) was calculated by E_{HOMO} and optical energy (E_g).[S3]

Internal quantum efficiency (IQE) simulation

The IQE of the devices was calculated by dividing EQE by the active layer absorption:

$$IQE(\lambda) = \frac{EQE(\lambda)}{A(\lambda)} \qquad \text{(S2)}$$

where $A(\lambda)$ is absorption of photons in the active layer of the device. To determine $A(\lambda)$, we performed transfer matrix model (TMM) simulations, using the measured optical constants, i.e., extinction coefficients (k) and refractive indexes (n), of the materials used in the solar cell stack.[S4] Two different methods were used to determine the optical constants. For the PEDOT:PSS and PNDIT-F3N interlayers, we used variable angle spectroscopic ellipsometry (VASE). The VASE measurements were performed on spin-coated thin films of PEDOT:PSS and PNDIT-F3N on top of silicon substrates. The incident angles used for the measurments were varied in steps of ten degrees from 45° to 75°. The software Complete Ease from J.A. Woolam Co., Inc was used to model the VASE measurement results. A Cauchy model was used for the transparent infrared spectral region to determine the thicknesses of the thin films. Tauc-Lorentz oscillators were used to model the optical constants. To determine the optical constants of the active layer materials, we used an ultraviolet-visible (UV-vis) spectrophotometer. The transmission (T) and reflection (R) spectra of the active layer films with different thicknesses were measured using the integrating sphere of the Perkin-Elmer lambda 950 spectrometer, and the n, k values of the active layers were determined by the transfer matrix formulism.

Transient grating ultrafast photoluminescence spectroscopy (TG-UFPL)

For the detection of the time-resolved emissive states, a home-built transient grating ultrafast photoluminescence technique was used.[S5] The setup was pumped with a femtosecond (< 150 fs) Ytterbium fiber laser (Tangerine SP, Amplitude Systemes; operating at 58 kHz, centred at 1030 nm). The output of the laser was split into the pump and gate parts. The pump

was frequency doubled to 515 nm using a home-built setup and focused to a spot (60 μm × 60 μm) at the sample. The sample's PL signal was collected and refocused onto a gate medium (1 mm fused silica crystal). The gate part of the beam was split using a 50/50 beam splitter to generate two gate beams. These beams then focused onto a gate medium at a crossing angle of 8° and overlapped with the PL signal using BOXCAR geometry. The spatial and temporal overlap of the gate beams inside a gate medium created a laser-induced transient grating, acting like an optical shutter to resolve the broadband PL signals. The gated PL signals were measured by an intensified CCD camera (Princeton instruments, PIMAX3). The time delay between the pump and the gate beams was controlled via a motorized delay line. The films were mounted under vacuum for each measurement.

Transient absorption spectroscopy (TAS)

TAS measurements were performed using a home-built experimental setup.[S6] The main light source was a Ti:Sapphire laser (SpectraPhysics) with pulse durations of 100 fs, at the repetition rate of 3 kHz, and centred at 800 nm. The 620 nm excitation pulses were generated using an optical parametric amplifier (TOPAS-C). The pump pulses were chopped at 1.5 kHz, half the fundamental repetition rate. The photoinduced changes in the absorption were then probed with a broadband supercontinuum pulse generated by focusing a portion of the fundamental to an yttrium aluminium garnet (YAG) crystal. The pump and the probe were overlapped in space and time at the sample, with the pump spot size of 350 μm × 350 μm. The variable delay stage was used to obtain the information about the excited state as a function of time after the excitation. After passing through the sample, the probe pulse was

spectrally dispersed using a prism and them collected using a CMOS camera (UV-visible components) and an InGaAs photodiode array (NIR components). The films were mounted under vacuum for each measurement.

Space charge limited current (SCLC) measurement

Hole-only and electron-only devices were fabricated using the architectures of ITO glass/PEDOT:PSS/active layer/Au for holes and ITO glass/ZnO/active layer/BCP/Ag for electrons. For hole-only devices, the pre-cleaned ITO glass was treated by UVO chamber for 15 min. Then PEDOT:PSS (*ca*. 30 nm) was spin-coated on it, and baked at 150 °C in the drying oven for 15 min. The photoactive layer was spin-coated at 3000 rpm on PEDOT:PSS layer, and Au (*ca*. 80 nm) was evaporated onto the photoactive layer under vacuum. For electron-only devices, ZnO (*ca*. 30 nm) was spin-coated onto the ITO glass, then the photoactive layer was spin-coated at 3000 rpm onto the ZnO layer. After that, BCP solution (0.5 mg mL^{-1} in ethanol) was spin-coated onto the active layer, followed by annealing at 80 °C for 5 min. At the end, Ag electrode layer (*ca*. 80 nm) was evaporated under vacuum. The mobility was extracted by fitting the *J*-*V* curves using SCLC method.[S7] The *J*-*V* curves of the devices were plotted as $\ln(Jd^3/V^2)$ versus $(V/d)^{0.5}$. The equation is as follows:

$$\ln\left(\frac{Jd^3}{V^2}\right) \cong 0.89(1/E_0)^{0.5}(V/d)^{0.5} + \ln(9\varepsilon_0\varepsilon_r\mu/8) \qquad \text{(S3)}$$

where J refers to the current density, μ is hole or electron mobility, ε_r is relative dielectric constant (*ca.* 3), ε_0 is dielectric constant of free space (8.82×10^{-12} F m^{-1}), $V = V_{appl} - V_{bi}$, where V_{appl} is the applied voltage to the device, and V_{bi} is the built-in voltage due to the

difference in work function of the electrodes (for hole-only diodes, V_{bi} is 0.2 V; for electron-only diodes, V_{bi} is 0 V). E_0 is characteristic field, and d is the thickness of the active layer.

Temperature-dependent SCLC measurement

A Cryo Industries Liquid Nitrogen Dewars with Lake Shore model 335 cryogenic temperature controller was used to modulate the operating temperature of devices. We waited 10 min after the temperature of system reached the target value, to ensure the device temperature stabilized. The cooling and heating rates were set as ~ 5 and ~ 2 K min^{-1}, respectively. Charge mobilities were obtained by using Keithley 2400 source-measure unit and electrochemical workstation (CH Instruments Model 1000C) under the dark. The *J-V* curves were fitted using SCLC method with the same device structure in traditional SCLC measurements.

Organic field-effect transistor (OFET) measurement

For bottom gate–bottom contact devices, Au and Ti layers were thermally evaporated onto a SiO_2/c-Si substrate using a shadow mask to form the source and drain contacts. The channel length and channel width were 10 μm and 1.4 mm, respectively. The substrate was thoroughly cleaned by placing it in piranha solution. After removing the piranha solution and rinsing the substrate with deionized water three times, the substrate was sonicated with deionized water, toluene, and isopropanol for 5 minutes, respectively. After drying the substrate with nitrogen, UV-ozone treatment was performed for 15 min, and then baked at 90 °C for 0.5 h at 0.1 Pa in a vacuum oven. Octyl trichlorosilane (OTS) treatment was performed by placing the cleaned substrate in OTS vapor for 2 h at 120 °C in the vacuum environment. The OTS-treated

substrate was ultrasonically treated with n-hexane, chloroform, and isopropanol for 5 minutes, and then was blown dry. PM6, AC174 and PM6:5%AC174 were dissolved in chloroform (10 mg mL^{-1} in total). Then the polymer solution was spin-coated on the processed substrate at 2000 rpm for 60 s, then annealed at 100 °C on the hot platform for 5 min. The devices were characterized using Keithley 4200-SCS semiconductor parameter analyzer in the nitrogen environment. The threshold voltage (V_T) and field-effect mobility (μ) in the saturation region were determined from

$$I_{DS} = (\frac{W}{2L})C_i\mu(V_{GS} - V_T)^2 \quad \text{(S4)}$$

where I_{DS} is the current density between drain and source, V_{GS} is the voltage between gate and source, W and L are the channel width and length, respectively, and C_i is the capacitance of the insulator.

Morphological characterization

Transmission electron microscopy (TEM) characterization was carried out on a JEM-2100 transmission electron miscroscope operated at 200 kV. Atomic force microscopy (AFM) characterization was performed using a Multimode 8 scanning probe microscope (Bruker Daltonics) in the non-contacting mode. Grazing incidence wide-angle X-ray scattering (GIWAXS) measurements were performed at beamline 7.3.3 at the Advanced Light Source (ALS).[S8] The 10 keV X-ray beam was incident at a grazing angle of 0.12°~0.16°. The scattered X-rays were detected using a Dectris Pilatus 2M photon counting detector (Switzerland). Grazing incidence small-angle X-ray scattering (GISAXS) measurements were carried out at 19U2 SAXS beamline at Shanghai Synchrotron Radiation Facility, Shanghai,

China. The energy of the X-ray source was set to 10 keV (wavelength of 1.24 Å) and the incident angle was 0.15°.

Contact angle measurements

The surface energies of PM6, AC174, Y6, and PM6:5%AC174 were calculated from contact angle measurements using the Owens and Wendt equation:

$$\gamma_L(1 + cos\theta) = 2\sqrt{\gamma_S^d \gamma_L^d} + 2\sqrt{\gamma_S^p \gamma_L^p} \qquad \text{(S5)}$$

where, γ is the surface energy, θ is the contact angle, the subscripts L and S are liquid and sample, respectively. The subscripts d and p are the dispersion and polar components of the surface energy, respectively, $\gamma = \gamma_d + \gamma_p$.[S9] Here, water ($\gamma_d$ = 21.8 mN m^{-1}, γ_p = 51.0 mN m^{-1}) and diiodomethane (γ_d = 49.5 mN m^{-1}, γ_p = 1.3 mN m^{-1}) were used as the testing liquids.[S10]

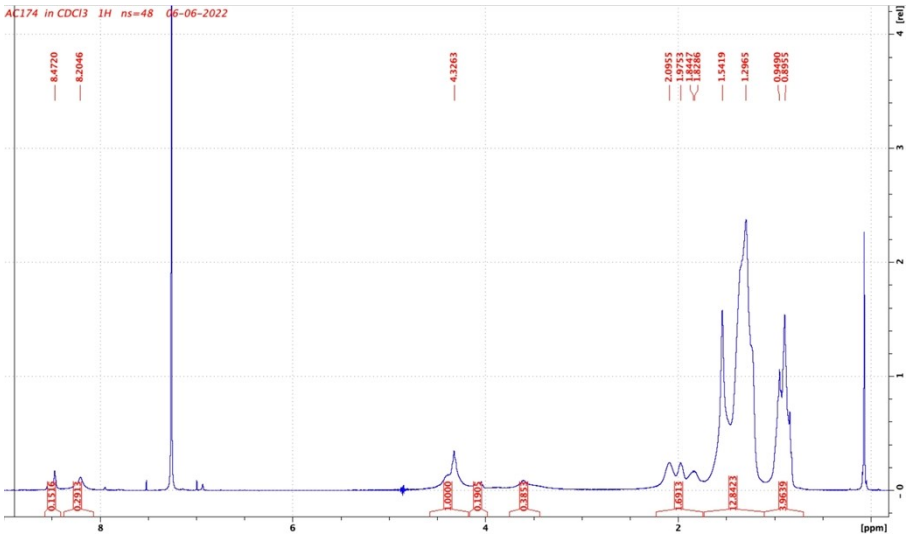

Fig. S1 NMR spectrum of AC174.

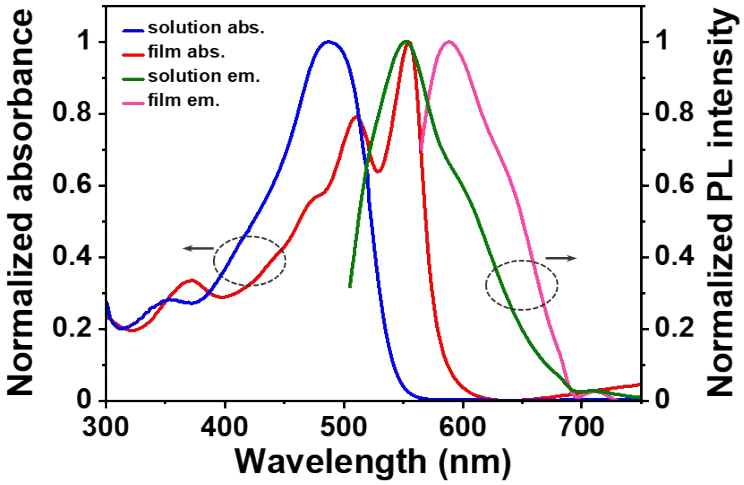

Fig. S2 Normalized light absorption spectra and normalized PL spectra of AC174 in dichloromethane solution and on thin film.

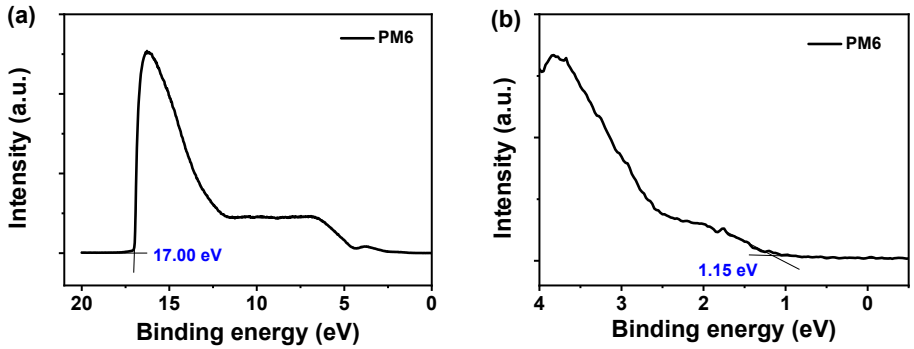

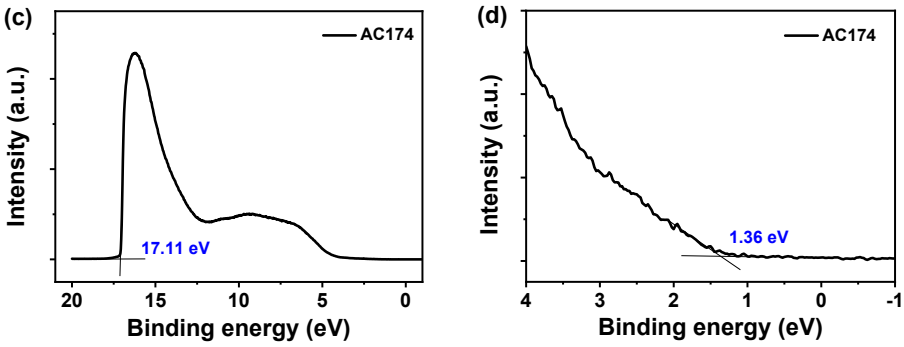

Fig. S3 UPS spectra of (a, c) the cutoff region and (b, d) the onset region of PM6 and AC174 films.

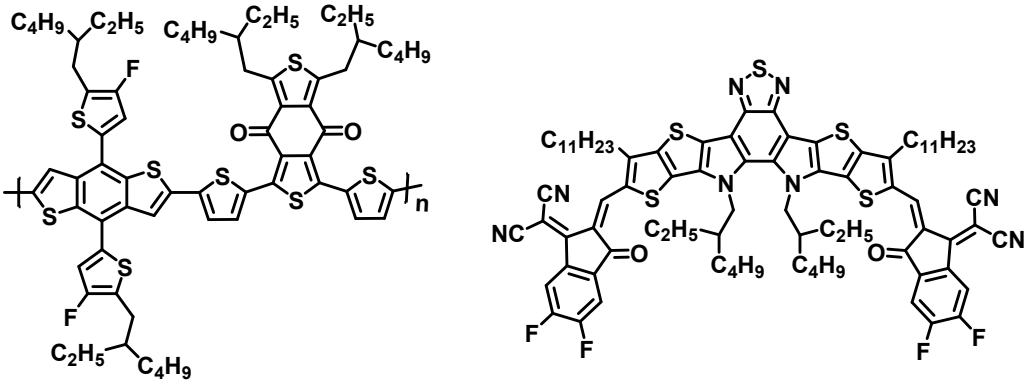

Fig. S4 Chemical structures of PM6 and Y6.

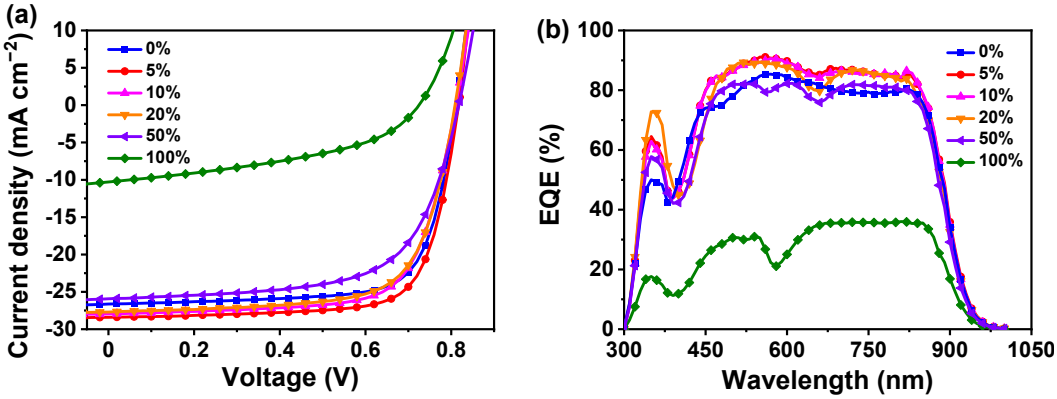

Fig. S5 (a) *J-V* curves and (b) EQE spectra of PM6:AC174:Y6 devices with different AC174 weight ratio in donors.

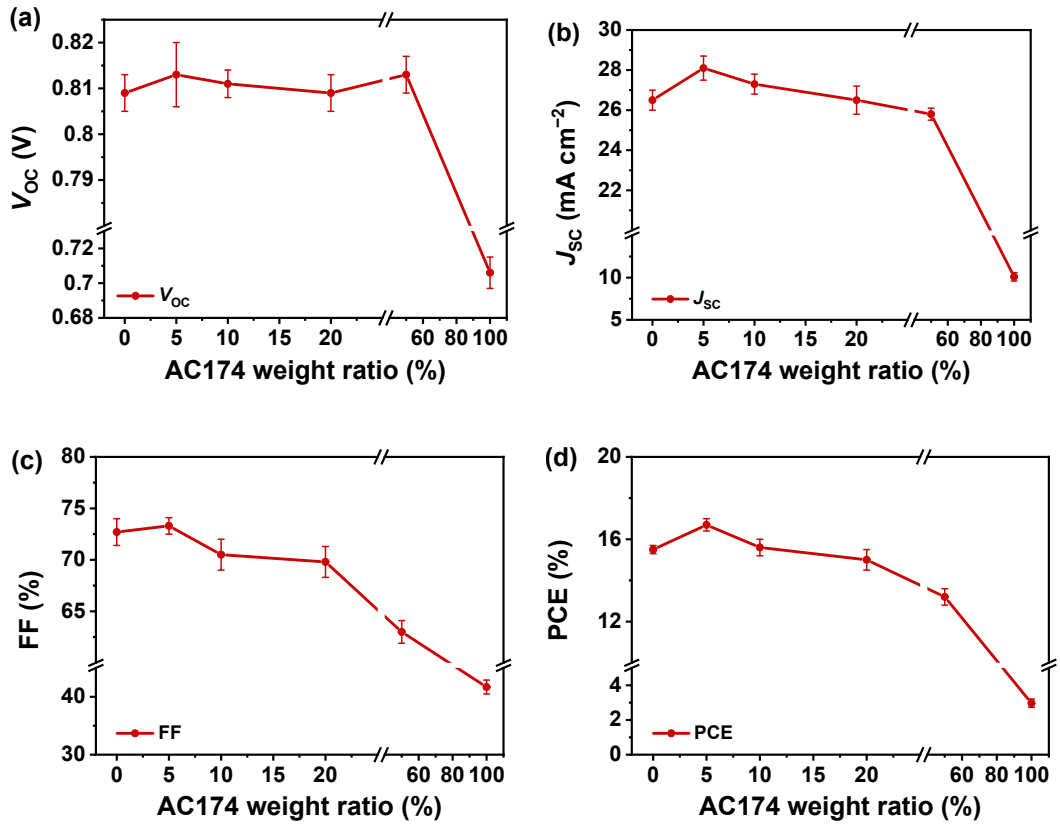

Fig. S6 (a) V_{OC}, (b) J_{SC}, (c) FF and (d) PCE as a function of AC174 weight ratio in donors.

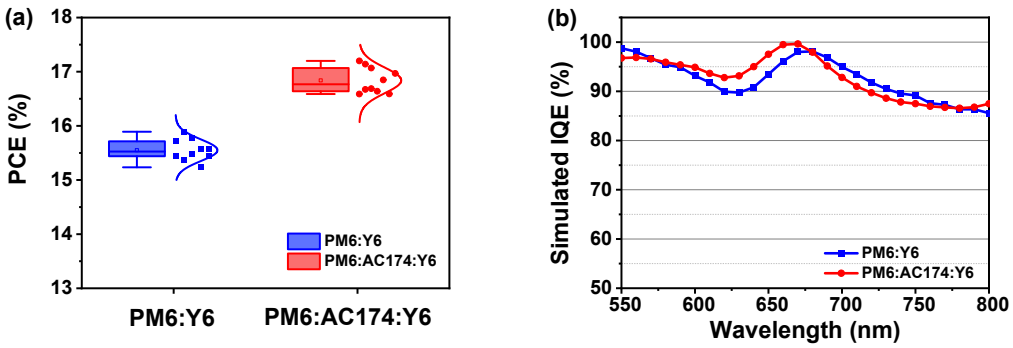

Fig. S7 (a) Statics of PCE distribution (The data were collected from 10 devices) and (b) simulated IQE curves of optimized PM6:Y6 and PM6:AC174:Y6 based devices.

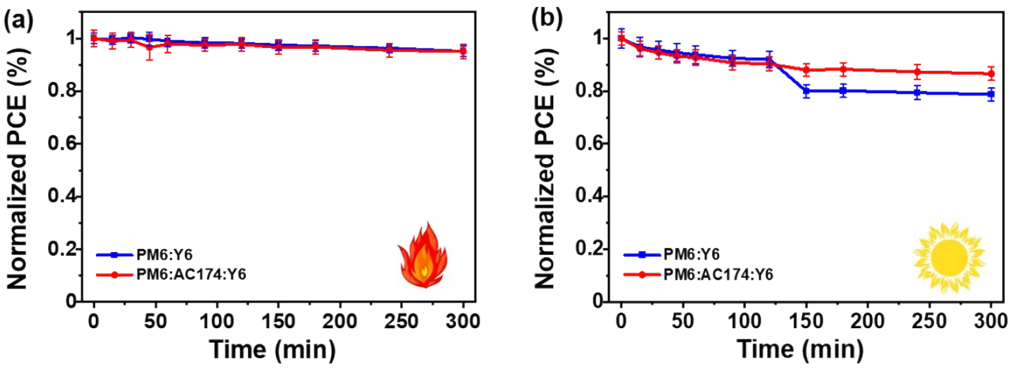

Fig. S8 (a) Heat stability curves and (b) light stability curves of PM6:Y6 and PM6:AC174:Y6 based devices.

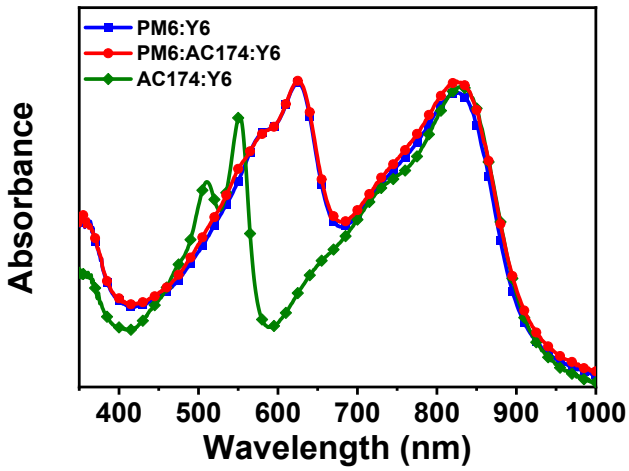

Fig. S9 UV-vis light absorption spectra of PM6:Y6, PM6:AC174:Y6 and AC174:Y6 blend films.

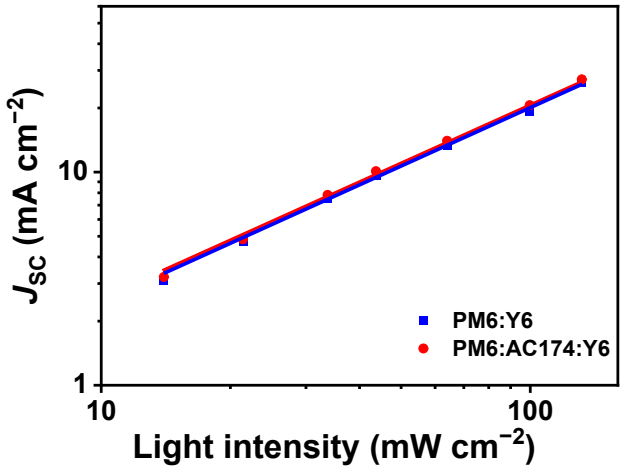

Fig. S10 J_{SC} versus light intensity of PM6:Y6 and PM6:AC174:Y6 based devices.

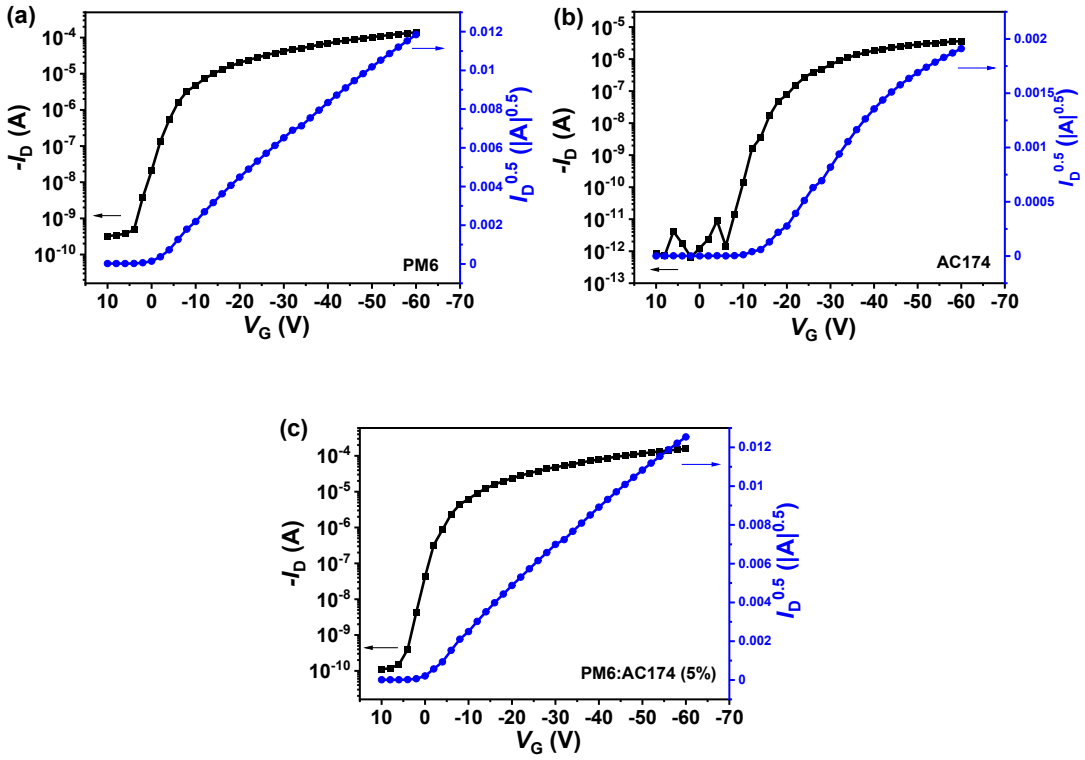

Fig. S11 Hole mobilities of (a) PM6, (b) AC174 and (c) PM6:AC174 films measured by OFET method.

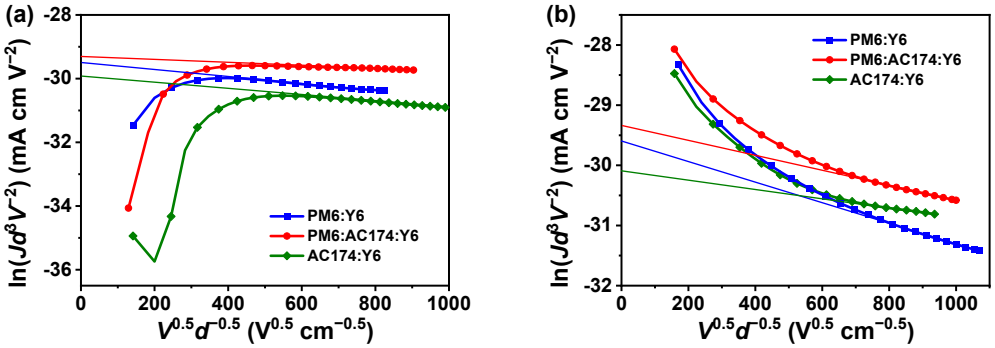

Fig. S12 *J-V* characteristics in the dark for (a) hole-only and (b) electron-only devices based on PM6:Y6, PM6:AC174:Y6 and AC174:Y6 films measured by SCLC method.

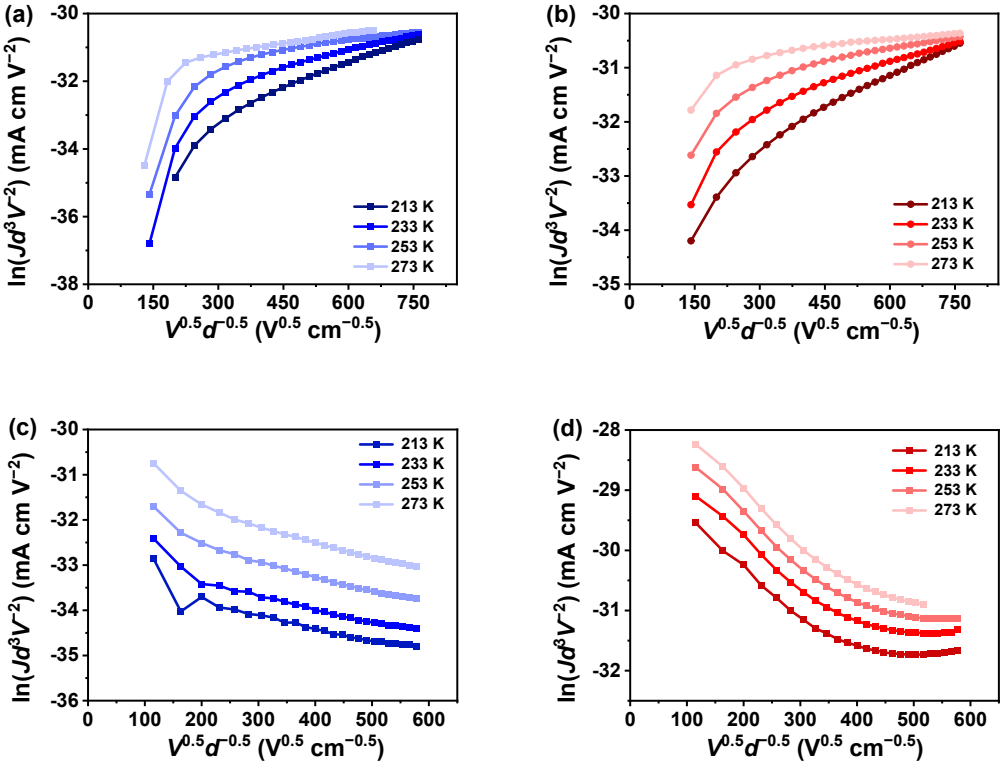

Fig. S13 Temperature dependence of hole transport for (a) PM6:Y6 film and (b) PM6:AC174:Y6 film. Temperature dependence of electron transport for (c) PM6:Y6 film and (d) PM6:AC174:Y6 film.

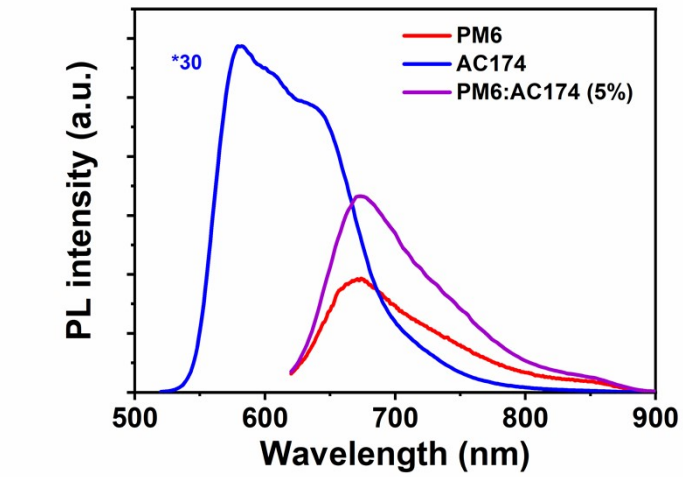

Fig. S14 PL spectra (real PL intensity of AC174 is 30 times of the value shown in Figure).

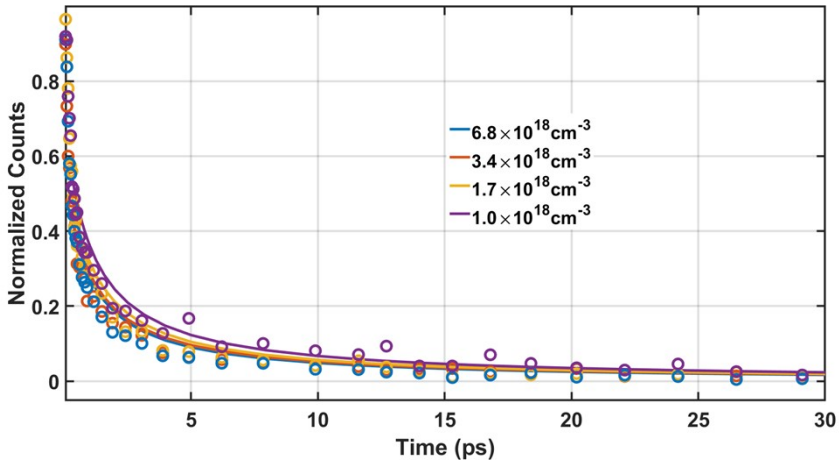

Fig. S15 Integrated photoluminescence emission kinetics of pure PM6 under difference excitation fluence.

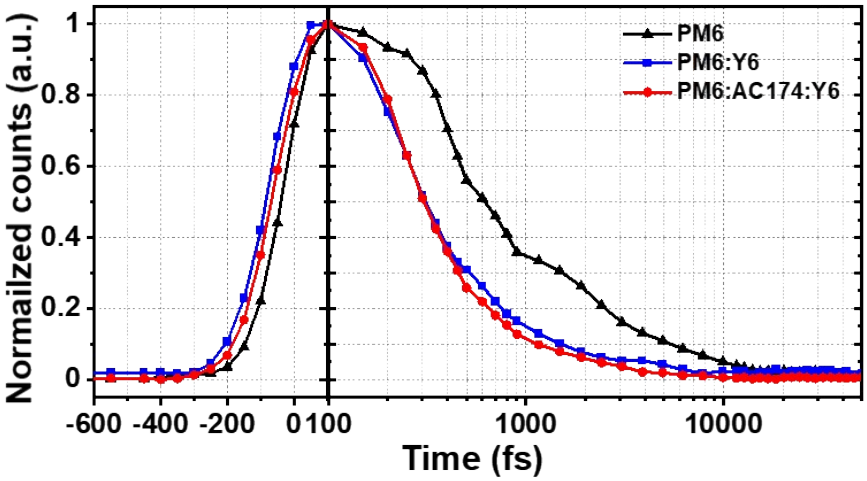

Fig. S16 Integrated photoluminescence emission kinetics of pure PM6, PM6:AC174 binary system, and PM6:AC174:Y6 ternary system.

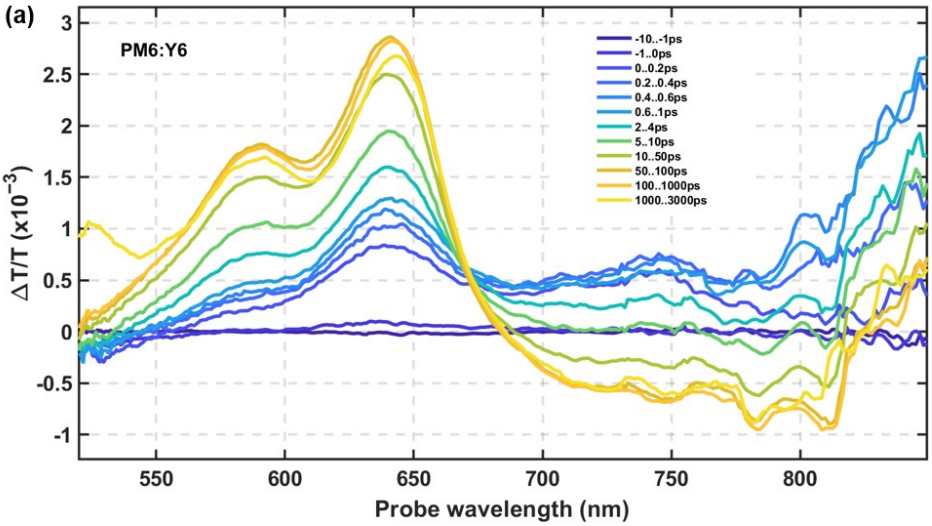

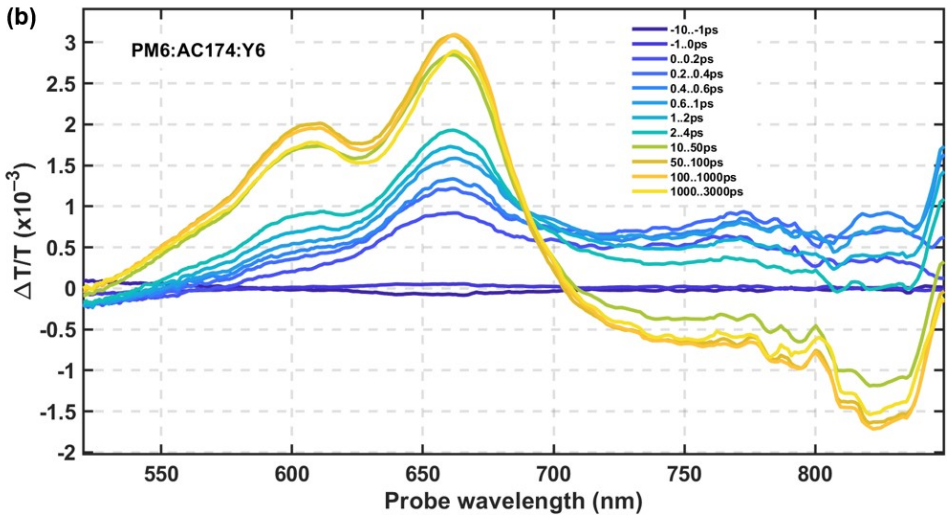

Fig. S17 Transient absorption spectra of (a) PM6:Y6 and (b) PM6:AC174:Y6 (5%) films using an 800 nm pump excitation with a fluence of 20 μW, for a range of time slices up to 3 ns.

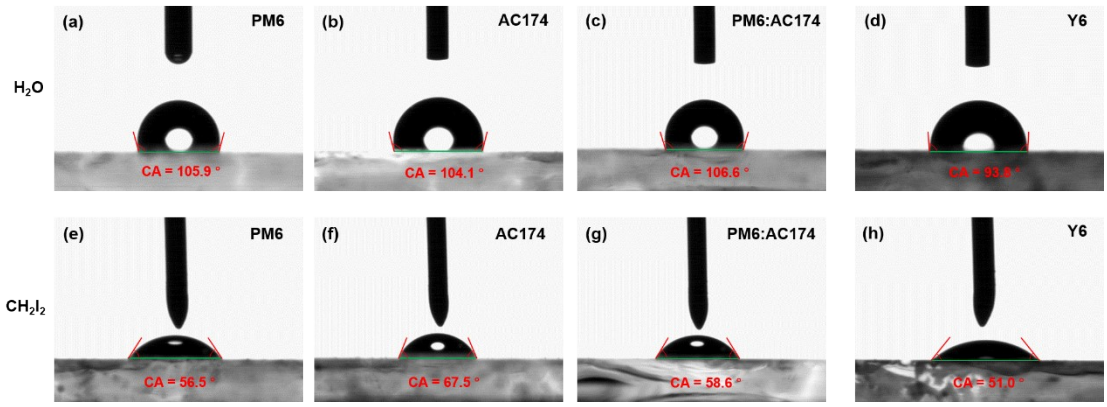

Fig. S18 Contact angles images of PM6, AC174, PM6:AC174 (5%), and Y6 films using water and diiodomethane as testing liquids.

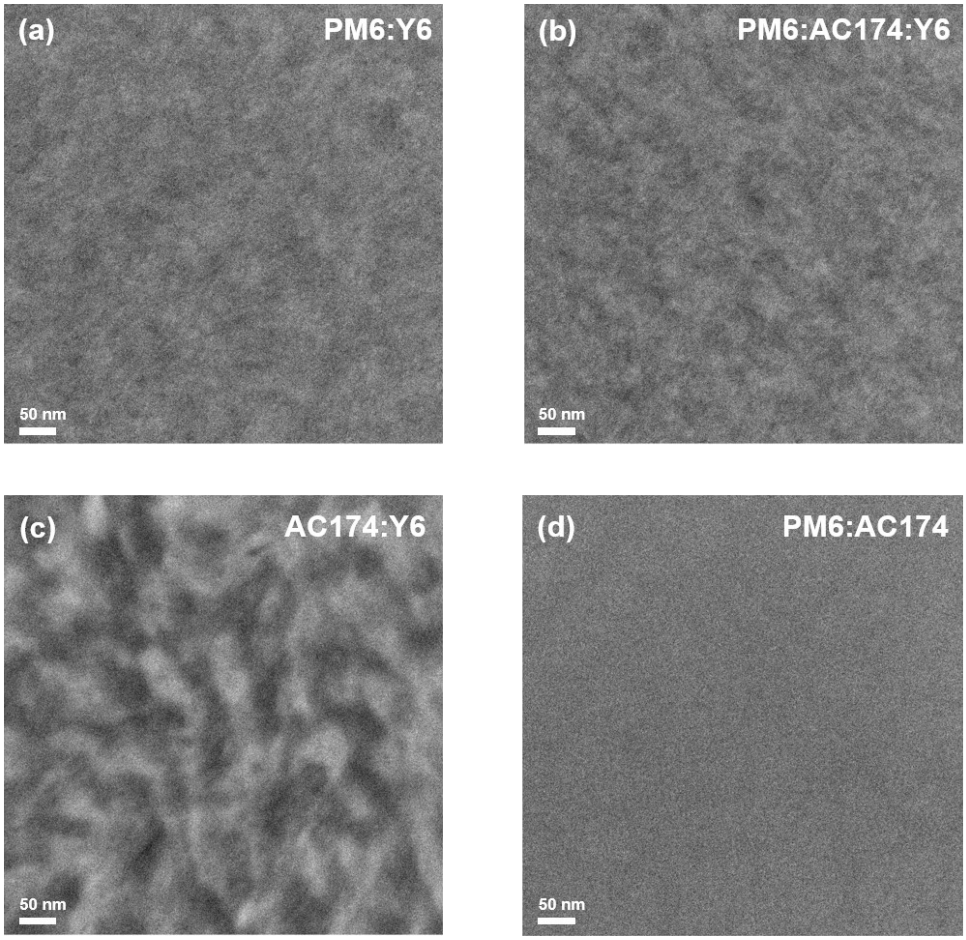

Fig. S19 TEM images of (a) PM6:Y6; (b) PM6:AC174 (5%):Y6; (c) AC174:Y6 (1:1.2) and (d) PM6:AC174 (5%) blend films.

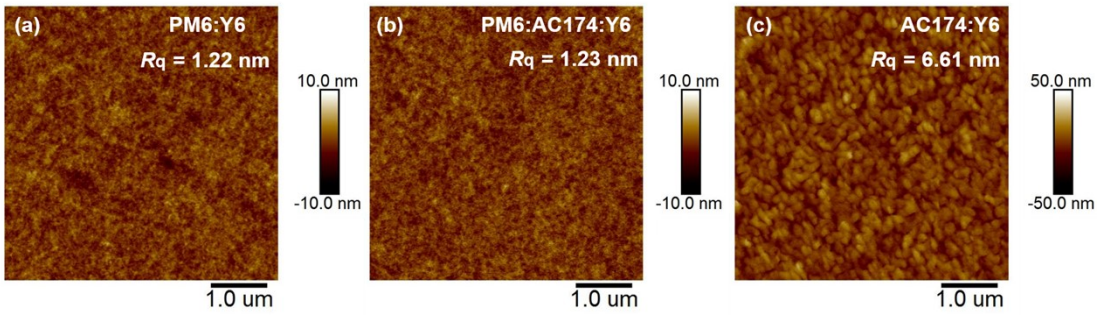

Fig. S20 AFM height images of (a) PM6:Y6; (b) PM6:AC174 (5%):Y6 and (c) AC174:Y6 (1:1.2) blend films.

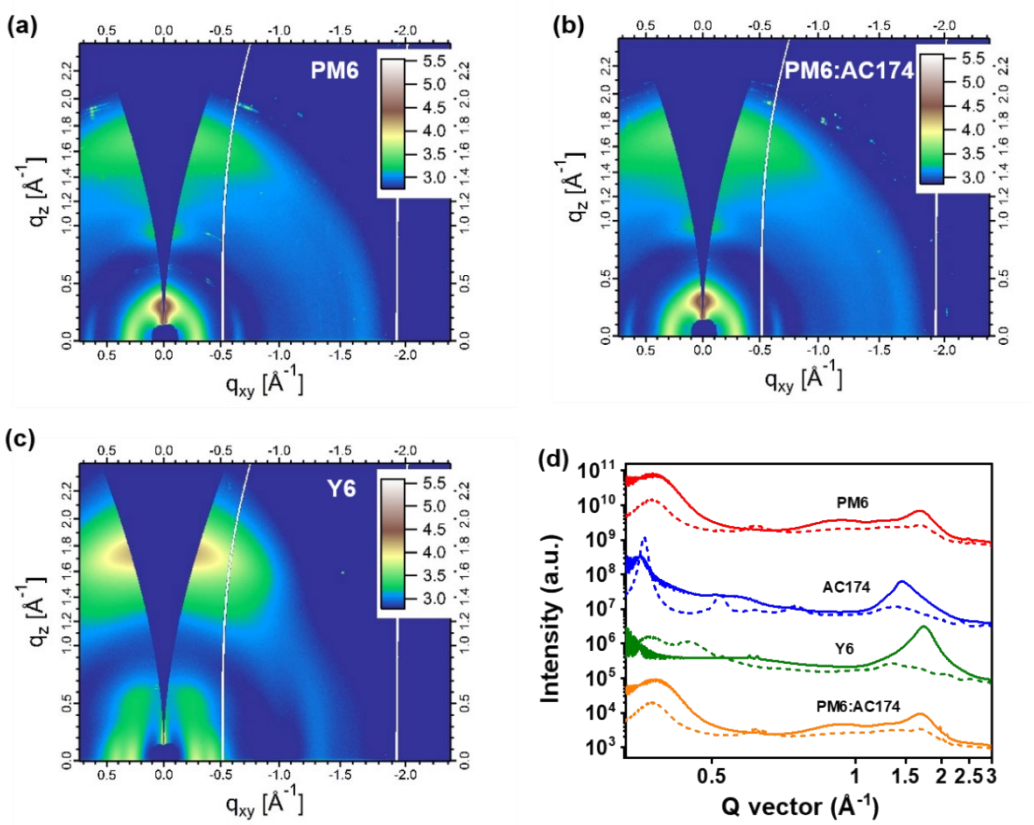

Fig. S21 2D GIWAXS patterns of (a) PM6, (b) PM6:AC174 (5%) and (c) Y6 films; (d) intensity profiles of PM6, AC174, PM6:AC174 (5%), and Y6 films along the out-of-plane (solid lines) and in-plane (dashed lines) directions.

Table S1 Performance of the OSCs with different amounts of AC174 in donors.[a]

AC174 content (%)	V_{OC} (V)	J_{SC} (mA cm^{-2})	FF (%)	PCE (%)
0	0.812 (0.809±0.004)	26.6 (26.4±0.5)	73.5 (72.7±1.3)	15.9 (15.5±0.2)
5	0.817 (0.813±0.007)	28.4 (28.1±0.6)	74.1 (73.3±0.8)	17.2 (16.7±0.3)
10	0.810 (0.811±0.003)	28.0 (27.3±0.5)	70.8 (70.5±1.5)	16.0 (15.6±0.4)
20	0.809 (0.809±0.004)	27.7 (26.5±0.7)	69.8 (69.8±1.5)	15.6 (15.0±0.5)
50	0.818 (0.813±0.004)	25.9 (25.8±0.3)	64.7 (63.0±1.1)	13.7 (13.2±0.4)
100	0.725 (0.706±0.009)	10.3 (10.1±0.5)	43.4 (41.7±1.2)	3.24 (2.97±0.24)

[a] Average values (in parenthesis) are obtained from 10 devices.

Table S2 Hole and electron mobilities of blend films.

Active layer	μ_h (cm^2 V^{-1} s^{-1})	μ_e (cm^2 V^{-1} s^{-1})	μ_h/μ_e
PM6:AC174:Y6	1.1×10^{-3}	1.1×10^{-3}	1.0
PM6:Y6	9.1×10^{-4}	8.3×10^{-4}	1.1
AC174:Y6	6.1×10^{-4}	5.1×10^{-4}	1.2

Table S3 Global fitting parameters of PM6 and PM6:AC174 (5%) fluence measurements.

Film	Parameter (excitation density)	Value	δ
PM6	k	1.83×10^{9}	
	n_1	1.0×10^{18}	4.54×10^{-7}
	n_2	1.7×10^{18}	5.44×10^{-7}
	n_3	3.4×10^{18}	5.89×10^{-7}
	n_4	6.8×10^{18}	6.39×10^{-7}
	Averaged δ		5.57×10^{-7}
PM6:AC174	k	1.53×10^{9}	
	n_1	1.0×10^{18}	
	n_2	1.7×10^{18}	
	n_3	3.4×10^{18}	
	n_4	6.8×10^{18}	
	-	δ	1.44×10^{-6}

Table S4 Contact angles and surface tensions of PM6, AC174, PM6:AC174 (5%) and Y6 films.

Compound	Contact angle（°）		γ_d (mN m^{-1})	γ_p (mN m^{-1})	γ (mN m^{-1})
	H_2O	CH_2I_2			
PM6	105.9	56.5	31.29	0.01	31.30
AC174	104.1	67.5	23.86	0.44	24.30
PM6:AC174	106.6	58.6	30.19	0.04	30.23
Y6	93.8	51.0	32.68	1.04	33.72

References

S1. Y. Zhu, R. D. Champion and S. A. Jenekhe, *Macromolecules*, 2006, **39**, 8712-8719.

S2. A. Sanzone, A. Calascibetta, M. Monti, S. Mattiello, M. Sassi, F. Corsini, G. Griffini, M. Sommer and L. Beverina, *ACS Macro Lett.*, 2020, **9**, 1167-1171.

S3. Y. Wang, B. Jia, J. Wang, P. Xue, Y. Xiao, T. Li, J. Wang, H. Lu, Z. Tang, X. Lu, F. Huang and X. Zhan, *Adv. Mater.*, 2020, **32**, 2002066.

S4. L. A. A. Pettersson, L. S. Roman and O. Inganäs, *J. Appl. Phys.*, 1999, **86**, 487-496.

S5. K. Chen, J. K. Gallaher, A. J. Barker and J. M. Hodgkiss, *J. Phys. Chem. Lett.*, 2014, **5**, 1732-1737.

S6. U. Megerle, I. Pugliesi, C. Schriever, C. F. Sailer and E. Riedle, *Appl. Phys. B*, 2009, **96**, 215-231.

S7. G. G. Malliaras, J. R. Salem, P. J. Brock and C. Scott, *Phys. Rev. B*, 1998, **58**, 13411-13414.

S8. A. Hexemer, W. Bras, J. Glossinger, E. Schaible, E. Gann, R. Kirian, A. MacDowell, M. Church, B. Rude and H. Padmore, *J. Phys.: Conf. Ser.*, 2010, **247**, 012007.

S9. D. K. Owens and R. C. Wendt, *J. Appl. Polym. Sci.*, 1969, **13**, 1741-1747.

S10. J. Wang, R. Zhu, S. Wang, Y. Li, B. Jia, J. Zhou, P. Xue, S. Seibt, Y. Lin, Z. Xie, W. Ma and X. Zhan, *Aggregate*, 2021, **2**, e29.